# Cement interface and bone stress in total hip arthroplasty: relationship to head size

M.T. Alonso-Rasgado[1], J.F. Del-Valle-Mojica[1], D. Jimenez-Cruz[1] C.G. Bailey[2], T.N. Board[3]

[1]*Bioengineering Research Group, School of Materials, The University of Manchester, Manchester, United Kingdom.*
[2]*Queen Mary University of London, London, United Kingdom*
[3]*Wrightington Hospital, Wigan and Leigh NHS Foundation Trust, Lancashire, United Kingdom.*

Author contribution:
All the authors contribute equally to this paper.

Corresponding Author:

Professor M.T. Alonso-Rasgado[1]
Professor of Biomaterials
School of Materials
University of Manchester
Pariser Building
Manchester
M13 9PL
UK
Tel: 0161 306 3857
email: teresa.rasgado@manchester.ac.uk

**Abstract**

The use of larger prosthetic femoral heads in total hip arthroplasty (THA) has increased considerably in recent years in response to the need to improve joint stability and reduce risk of dislocation. However, data suggests larger femoral heads are associated with higher joint failure rates. For cemented implants, ensuring the continued integrity of the cement mantle is key to long term fixation. This paper describes an investigation into the effect of variation in femoral head size on stresses in the acetabular cement mantle and pelvic bone. Three commonly used femoral head sizes: 28 mm, 32 mm and 36 mm diameter were investigated. The study was undertaken using a finite element model validated using surface strains obtained from Digital Image Correlation (DIC) during experimentation on a composite hemipelvis implanted with a cemented all-polyethylene acetabular cup.

Following validation, the models were used to investigate stresses in the pelvic bone and acetabular cement mantle resulting from two loading scenarios; an average weight subject (700 N) and an overweight subject (1000 N) undertaking a single leg stand.

We found that the highest peak stresses occurred in the anterosuperior and posterosuperior regions of the bone-cement interface, in the line of action of the load, where debonding usually initiates. Stress on the cortical bone-cement interface increased with femoral head diameter by up to 9% whilst stresses in the trabecular bone remained relatively invariant. Our findings may help to explain higher joint failure rates associated with larger femoral heads.

**Number of words: 242**

**Key Words**: finite element, total hip arthroplasty, femoral head, cement mantle

## Introduction

Total hip arthroplasty (THA) is a highly effective method for the treatment of a variety of hip pathologies such as osteoarthritis and avascular necrosis of the femoral head [1]. In the UK alone, The National Joint Registry for England, Wales and Northern Ireland (NJR), reported that a total of 890,681 THA were performed between 2003 and 2016, making THA the second most common joint surgery during that period [2].

Between 2003 and 2016 the use of larger femoral head sizes with cemented and cementless acetabular cups gained popularity in the UK [1, 2, 3]. Larger femoral heads are used by surgeons in order to increase joint stability and reduce the risk of dislocation [1, 4, 5]. In 2003, the standard head size of 28 mm was used in 73% of hip replacement procedures in the UK; this number fell to 29% in 2016. Femoral head sizes of 32 or 36 mm were used in a combined total of 5.5% of all hip replacement procedures in 2003; by 2016 this figure had risen to 70% [2, 3]. Despite improvements in joint stability and reduced risk of dislocation, it has recently been reported that, for cemented acetabular cups, 36 mm femoral heads appear to be associated with higher joint failure rates than smaller heads [2].

Reasons for revision following primary hip surgery include femoral or acetabular component loosening, dislocation, periprosthetic fracture and infection. The integrity of the acetabular component, for cemented implants, depends on the integrity of the cement mantle [6]. Failure of the mantle may lead to aseptic loosening of the acetabular component, one of the main causes of implant failure [6,7]. Failure generally initiates as demarcation and fibrous tissue formation at the cement-bone interface, most commonly observed as radiolucent lines on radiographs in the superior portion of the acetabular rim where the largest stresses in the bone and cement occur [8,9], zone 1 of the DeLee and Charnley system [8]. The demarcation

region at the bone-cement interface is associated with subsequent bone resorption that leads to cup migration and final gross-loosening [7, 10]. Higher stresses within the cement mantle will decrease its life under cyclic loading with failure occurring at the region of greater stress [7,11].

The mechanical behaviour within the cement mantle and at the bone-cement interface, where debonding usually initiates [6], is affected by multiple factors including cement thickness [7,12], acetabular cup outer diameter [12, 13], cup penetration [7, 13, 14] and inclination angle [13, 14], bone quality [12], body mass index [12] and femoral head size [12,15].

To date, investigations into the use of different femoral head sizes in THA have focussed primarily on joint stability aspects [16] with limited research undertaken into the effect of head diameter on stress distribution in the cement mantle and pelvic bone. Hoeltzel *et al* [16] determined the effect of femoral head size on the deformation of ultrahigh molecular weight polyethylene acetabular cups. They found that peak strain values on the surface of the acetabular cup increased with increasing femoral head size above 26 mm. Based on this, the authors predicted a maximum tensile stress level of 7.75 MPa in the cement mantle. Lamvohee *et al* [12] used finite element reconstructed hemi-pelvis to investigate the effect of prosthetic femoral head implant sizes of 22 and 28 mm on the stresses developed in the acetabular cup and in uniform thickness cement mantles for different bone qualities They found that the tensile stress in the cement mantle increased by 17 – 23% when the larger femoral head (28 mm) was employed, compared to the smaller head (22 mm), whereas stresses in the acetabular components decreased.

In order to address the current gap in knowledge regarding larger femoral head sizes and

acetabular component integrity in cemented THA, this paper investigates the effect on stresses in the acetabular cement mantle and pelvic bone of using three femoral head sizes, 28 mm, 32 mm and 36 mm diameter, in THA. Two loading scenarios were considered, a person of average weight (700 N) and an overweight person (1000 N) undertaking a single leg stand.

## Materials and methods

Three Finite Element (FE) models simulating femoral head sizes of 28 mm, 32 mm and 36 mm diameter were developed from Computed Tomography (CT) scan data of an artificial hemipelvis implanted with a cemented acetabular cup. The models were validated with experimental work which consisted of comparing predicted surface strains from the 36 mm femoral head FE model with corresponding strains obtained experimentally on a fourth generation Sawbones® composite hemipelvis, loaded to simulate the one leg stand activity of an average patient with a body weight of 700N. Following validation, the models were used to investigate stresses in the pelvic bone and (non uniform thickness) acetabular cement mantle for the three femoral head sizes under two loading scenarios; an average weight subject (700 N) and an overweight subject (1000 N) undertaking a single leg stand. Figure 1 summarises the methodology used for this study.

Three main regions, A1 and A2 at the pelvic bone and A3, the cement mantle interfaces, were considered in the stress analysis (Figure 2). Regions A1, A2 correspond to the superior and anterior periacetabular areas respectively. The periacetabular bone region is located within the predominant area of the reaction force transfer at the hip joint [14]. Region A3 constitutes the acetabular cement mantle interfaces (bone-cement-cup), which fix the implant to the pelvic bone; this region is where bone-implant load transfer occurs [17, 18]. Failure at

the bone-cement interface in this region can lead to aseptic loosening of the acetabular component and ultimately implant failure [14].

**Finite Element Model**

Three FE models were constructed from CT scan data of an artificial composite fourth generation Sawbones® (AG, Sweden) hemipelvis implanted with a cemented all-polyethylene acetabular cup with an outer diameter of 50 mm and inner diameter of 36.5 mm to accommodate a 36 mm femoral head (Figure 3(a)).

Firstly, segmentation masks for the pelvic bone and cement mantle were created from the CT scan data (vol files) using 3D visualisation and analysis software (Avizo (FEI Visualization Sciences Group, Berlin, Germany). The mask for the hemipelvis included both the cortical and trabecular bone sections and was exported as a set of 485 CT slices with a thickness of 0.5 mm, transverse resolution of 400 x 400, and pixel size of 0.5 x 0.5 mm. The non uniform thickness cement mantle mask was exported as a separate set of 181 CT slices of the same thickness, and resolution as the hemipelvis mask. Each set of CT slices was imported into 3D image segmentation and processing software in order to generate the 3-D surface of the cortical and trabecular bone regions and the cement mantle (Figure 3(b)).

The cortical and trabecular bone and cement mantle 3-D geometries were then exported in IGES file format and imported into Abaqus 6.13 (Dassault Systemes, RI, USA). The acetabular cup and femoral head geometries were created in Abaqus 6.13 (Figure 3(c,d)) and the full model then assembled and meshed (Figure 3(e)). The cement mantle, cortical and trabecular bone were meshed with quadratic tetrahedral elements (C3D10) as this type of element produces meshes that better represent complex geometries such as bony structures.

The acetabular cup and femoral head were meshed with quadratic hexahedral elements (C3D20R) as both components are of regular geometric shape and so can be accurately represented using hexahedral elements. Hexahedral elements are recommended whenever possible to avoid distorted meshes.

*Boundary conditions*

The hemipelvis was fully fixed with displacements/rotations defined as zero in all directions (Figure 4) at the sacro-iliac joint and pubis symphysis [7,14,19,20]. The cement-bone and cement-cup interfaces were considered as fully bonded [21]. The contact between femoral head and acetabular cup was defined as a surface-to-surface contact interaction with frictionless tangential behaviour [14,20]. A load of 1800 N was applied as a concentrated force at the central node of the femoral head to simulate the peak reaction force (RF) at the hip joint during a one leg stand activity for the average subject [22].

*Materials*

The FE model considered composite synthetic fourth generation Sawbones® cortical and trabecular bone; the mechanical properties of the synthetic bone were provided by the manufacturer. Cross linked ultra high molecular weight polyethylene (UHMWPE), steel and acrylic bone cement were also considered in the model for the acetabular cup, femoral head and cement mantle, respectively. Linear and elastic isotropic behaviour was assumed for all the materials. The properties of the acrylic bone cement, UHMWPE, and steel were assigned in accordance with those reported in the literature [17,18] (Table S-1, see Supplementary Material) shows all the material properties used in the models.

*Mesh sensitivity*

To ensure accuracy of the results, a mesh sensitivity analysis was first undertaken. The

analysis consisted of altering the density of the tetrahedral element mesh (C3D10) in the bone and (non uniform thickness) cement mantle and the density of the hexahedral elements (C3D20R) in the implant head and acetabular cup for the three head sizes (28 mm, 32 mm and 36 mm) for the loading condition of an average subject undertaking a one leg stand.

The stress predicted in the bone and cement mantle was compared for three different mesh densities: coarse, medium and fine (Table S-2, see Supplementary Material). The medium mesh density was chosen for all components as the predicted stresses in the bone and cement mantle varied by less than 1% compared with the fine mesh.

**Validation of the finite element model: experimental work**

To validate the FE model, experimentation was undertaken on a fourth generation Sawbones® composite hemipelvis. A cemented all-polyethylene acetabular cup with a 50 mm inner and 36.5 mm outer diameter was implanted in the composite hemipelvis by an orthopaedic surgeon. Application of a reaction force of 1800 N at the hip joint corresponding to a one leg stand activity of an average subject with a body weight of 700 N was then simulated using a stainless-steel ball bearing of 36 mm diameter and Digital Image Correlation (DIC) was used to record vertical surface strains. For validation purposes and to ensure accurate Digital Image Correlation (DIC) vertical surface strain measurements, two sub-regions A1-1 (300 $mm^2$) and A1-2 (250 $mm^2$) were defined within region A1 (1330 $mm^2$), the superior periacetabular area of the hemipelvis (Figure 2).

*Experimental setup*

Loading was applied using a single column universal materials testing system (Instron 3342,

Instron, MA, USA). The loads at the inner surface of the acetabular cup were applied using a 2 kN load-cell using a 36 mm stainless-steel ball bearing attached by employing a custom-made steel taper (Figure 5(a)). A holding device consisting of a clamp for the fixation of the sacro-iliac joint (Figure 5(a)), and a support for fixation of the pubis symphysis (Figure 5(b)) was used to position and secure the synthetic hemipelvis. The position of the hemipelvis was set in order to apply the load at an angle of 6.5º as shown in Figure 4(b). A system consists of an array of two 5 megapixels cameras with a 12 mm focal length, computer interface for data acquisition and data processing software (Figure 5(a)) was used to obtain the vertical surface strains of the pelvic bone.

*Experimental procedure*:

A speckle pattern was created over the surface of the synthetic hemipelvis by applying black paint sprayed sparsely over a previously painted base layer of white paint. Once the speckle pattern was created, the synthetic hemipelvis was secured in the universal machine using the holding device and its position was adjusted so that the compressive axial load applied at the inner surface of the acetabular cup by the stainless-steel ball bearing was at an angle of 6.5º [22] with the vertical axis as shown in Figure 4(b).

Before measurements were taken, the DIC system was calibrated following the guidelines provided by manufacturer [23]. The cameras were then positioned to capture the image data at regions A1-1 and A1-2 at a distance of 280 mm from the test hemipelvis. Loading from 1200 N to 1800 N was applied in increments of 200 N; the loading cycle was repeated a total of 10 times.

Prior to each load application, an image of the initial state (unloaded/non-deformed); was captured. The load was then applied with a displacement control of 1 mm/min. Once the set

load was reached, a 3 minutes waiting period was observed for the system to stabilise, after which an image of the final state (loaded/deformed) was recorded. When all the measurements for regions A1-1 and A1-2 were completed, the cameras were positioned to take measurements at region A2. The cameras were set at the same distance from the subject as for the measurements of region A1-1 and A1-2 and the same procedure of loading and image data recording was followed.

*Data Processing*

Once the image data of the initial and final states for regions A1-2, A1-2 and A2 was recorded for each load application, computation of the image data of was carried out in Aramis V6.1 (GOM Ltd, Athlone, Ireland), the software used for data capture and processing for the Digital Image Correlation (DIC) system. To compute the vertical surface strains, a strain computation mask with quadrangular facets of 20 pixels x 20 pixels and a step between facets of 10 pixels was created over the surface of the composite hemipelvis. A linear strain computation algorithm in Aramis V6.1 was used to calculate the vertical surface strains.

An average noise filter was applied to the post-processed data to eliminate any possible measurement noise. The average vertical surface strain within regions A1-1, A1-2 and A2 was calculated using the statistic tool within Aramis V6.1; the value was recorded for each of the 10 measurements taken for each load (1200 N, 1400 N, 1600 N, 1800 N), and the average of the 10 measurements was calculated and used to compare against the FE model predictions.

The repeatability of the experimental measurements was evaluated by calculating the coefficient of variation (CV) for the measurements for regions A1-1, A1-2 and A2. A

maximum CV of 5% was calculated for regions A1-1, A1-2 and A2. The mean and standard deviation (Std. Dev.) was calculated for the ten vertical surface strain measurements taken at each load. The CV for each load case for all regions was then determined by calculating the ratio of the respective Std. Dev. to the mean.

*Contact area validation between stainless-steel ball bearing and inner surface of acetabular cup*

In order to investigate the contact pattern between the stainless-steel ball bearing and the inner surface of the acetabular cup, a thin layer of pigmented paste, commonly used to detect high spots on mating surfaces, was applied over the surface of the stainless-steel ball bearing. A load of 1800 N was applied at the inner surface of the cup as previously described. After the loading, a well-defined contact pattern was visible on the inner surface of the acetabular cup Figure 6.

Once the FE model with the 36 mm femoral head was validated, the 32 mm and 28 mm femoral head models were created by modifying the inner diameter of the acetabular cup from the 36 mm femoral head model to accommodate the smaller head sizes (Table S-3, see Supplementary Material). An investigation into the pelvic bone and cement mantle interfaces stresses (A1, A2, and A3) was then undertaken for the three femoral head sizes for loading conditions corresponding to average and overweight subjects undertaking a single leg stand. For the overweight subject, a load of 3600 N was applied to simulate the peak reaction force during the activity [22].

## Results

To aid analysis of the results from the bone-cement-cup interface each interface was divided into four quadrants, anterosuperior (1), posterosuperior (2), anteroinferior (3) and posteroinferior (4), of equal area of 1,120 mm².

### FE Model Validation: Vertical surface strains in regions A1 (A1-1, A1-2) and A2:

Table 1 and Table 2 show a comparison of the average vertical surface strains obtained from the FE model and experimental data at the superior A1 (A1-1, A1-2) and anterior A2 periacetabular regions, respectively. Good agreement was obtained between FE model predictions and experimental data, model predictions were within 5% of experimentally determined values in all cases. Figure 7 shows the femoral head force-displacement curve for the numerical and experimental models where upon inspection it can be seen that model predictions match experimental values closely, with the largest difference being around 4%.

In addition, a comparison was undertaken between the femoral head-acetabular cup contact area predicted by the FE model and that determined from the experimentation. Good agreement was obtained between the two: the FE model predicted a contact area of 393 $mm^2$ compared to 373 $mm^2$ ascertained from the experimentation, a difference of 5.3%.

### Bone stress.

*Pelvic bone: Regions A1 and A2*

Figures 8 and 10 show a comparison between predicted average von Mises stresses in the pelvic bone regions for the three femoral head sizes (28 mm, 32 mm, and 36 mm) for an average weight and overweight subject respectively. From these figures it can be seen that the highest average von Mises stresses occurred in the cortical bone of region A1, for the three femoral head sizes in both scenarios considered. For the 28mm and 32mm femoral heads, average von Mises stresses was 2.8 and 5.7 MPa in the cortical bone of region A1 for average and overweight subject respectively, for the 36 mm femoral head it was 2.9 and 5.8 MPa. The next highest stresses occurred in the cortical bone of region A2, 2.0 MPa (average subject) and 4.0 MPa (overweight subject) for all three femoral head sizes. Average von Mises stress was lower in the trabecular bone, 0.4 and 0.2 MPa (average subject) and 0.7 and 0.5 MPa (overweight subject) in regions A1 and A2 respectively, for all three femoral head sizes investigated. In general, the stress in regions A1 and A2 increased by approximately 100% in the overweight patient model.

**Cement interfaces: bone-cement and cup-cement**

A comparison of the predicted von Mises stresses on the two cement interfaces (bone-cement and cement-cup) for the three femoral head sizes considered are shown in Figures 9 and 11 for average and overweight subjects respectively. The highest stresses occurred in the cortical bone-cement interface in the superior quadrants (anterosuperior and posterosuperior) for both scenarios (average and overweight subject) and for all three femoral head sizes considered. For the average weight subject stresses on the cortical bone-cement interface range between 2.8-3.0 MPa for the anterosuperior quadrant and 2.6-2.8 MPa in the posterosuperior quadrant. In the case of the overweight subject stresses on the cortical bone-cement interface range between 5.8-6.3 MPa for the anterosuperior quadrant and 5.4-5.6 MPa in the posterosuperior

quadrant. Lower stresses were founded in the inferior quadrants (anteroinferior and posteroinferior) for all cases, with the lowest stress occurring in the trabecular bone-cement interface. In general, stresses increased with increasing femoral head diameter. Stresses in the cement-cup interface were generally higher than the stress in the trabecular bone-cement interface (by 17.6%, 17.6% and 11% for the 28mm, 32mm and 36mm head sizes respectively for the average weight patient and by 14.7%, 11.4% and 14.3% for the 28mm, 32mm and 36mm head sizes respectively for the overweight patient) but lower than those in cortical bone-cement interface (by 23%, 24% and 28.6% for the 28mm, 32mm and 36mm head sizes respectively for the average weight patient and by 27.8%, 29.5% and 28.6% for the 28mm, 32mm and 36mm head sizes respectively for the overweight patient).

Figure 12 shows how bone-cement-cup interface stress in the superior quadrants varies with loading condition and femoral head diameter. In general, stress increased slightly on both interfaces with femoral head diameter. Stress increased by approximately 100% between average weight and overweight subjects (when body weight increased from 700 N to 1000 N).

**Discussion**

The use of larger prosthetic femoral heads in THA has increased considerably in recent years [2,3] in response to the need to improve joint stability and reduce risk of dislocation. However, data suggests larger femoral heads are associated with higher joint failure rates [2]. This finding is further supported by an analysis of data from the Dutch Athroplasty Register between 2007 and 2015, which found that whilst the risk of dislocation was significantly lower for 36mm femoral heads, the overall risk of revision within 6 years was higher (3.2%)

than that for both 32 mm (2.7%) and 22-28mm (3.1%) heads [27]. Interestingly, femoral component related failure seemed to be the cause of the greatest revision burden for larger heads, however, the data was not broken down by fixation type although overall, uncemented fixation accounted for twice as many cases as cemented, being used in approximately 60% of primary cases compared to about 28% for cemented. Previous clinical studies have shown however, that the failure rate of the acetabular component is between two and four times higher than that of the femoral component after 10 years in vivo in cemented THA [7].

This paper has investigated the effect on stresses in the acetabular cement mantle and pelvic bone of using three femoral head sizes, 28 mm, 32 mm and 36 mm diameter, in THA.

Previous studies have determined that the majority of load transfer across the pelvic joint occurs through the cortical shell, predominantly in a thin strip in the anterosuperior edge of the acetabulum [24]. Predictions from our model are in accord with these findings. We found that the highest average von Mises stresses occurred in the cortical bone of the superior and anterior periacetabular area of the pelvis. In addition, predictions from our model indicated that pelvic bone stresses are not significantly affected by femoral head implant size, a similar finding to that of Lamvohee *et al* [12].

Our model predicts that average von Mises stresses on both the bone-cement and cement-cup interfaces increased, by up to 10%, with an increase in femoral head diameter (and subsequently a decrease acetabular cup thickness). In addition, when the body weight of the subject considered increased from 700N to 1000N, stresses on the cement mantle interfaces increased by approximately 100%.

The highest stresses in the cement mantle were found to occur in the superior quadrants (anterosuperior and posterosuperior) of the joint, in the line of action of the load, which is in accord with previous related studies [7,11,14]. In particular, the greatest stresses produced were on the cortical bone-cement interface. Previous investigations undertaken by Hua *et al* [14] and Coultrup *et al* [7] using computational prosthetic hip models had determined that maximum stresses within the cement mantle occur at the cup-cement interface. However, both of these prior studies represented the cement mantle using an idealised, constant thickness, hemispherical geometry. A constant thickness representation generates a gap on the bone-cement interface at the acetabular rim. In the actual surgical procedure, this gap is filled with bone cement by the surgeon. As our model was created from CT scan data of an artificial composite hemipelvis implanted with a cemented all-polyethylene acetabular cup by a surgeon, the cement mantle was irregular in thickness (average 4.7 mm, range 3.0 - 7.8mm) and the gap on the bone-cement interface at the acetabular rim was filled with bone cement, therefore better representing the real surgical case, enabling load to be transferred to the acetabular rim, unlike in the constant cement mantle thickness representation.

A uniform cement mantle layer is important for proper and long term fixation of the acetabular component in THA and a number of techniques have been proposed to aid in this respect; despite this, consistent thickness cement mantles remain difficult to reproduce [25, 26]. In surgical practice therefore, some variability in cement mantle thickness is inevitable; as such this is a strength of our model compared to those which assume a constant, uniform cement mantle thickness. It has been reported that stress variation across the thickness of the cement mantle is around 10% for a uniform 3.5 mm cement layer [11]. The results from our model compare well to this, with through thickness cement mantle stress variation predicted to be 8%.

Our finding, that the highest stresses in the cement mantle develop on the bone-cement interface, is significant as it has been determined that debonding at the bone-cement interface as a result of fatigue is the main failure mechanism responsible for acetabular replacement loosening [11]. In our model, average von Mises stresses on the bone-cement increased by up to 10% with femoral head diameter; this would cause a corresponding reduction in the fatigue life of the cement mantle [12], which may explain the higher joint failure rates associated with larger femoral head diameters [2]. Further, clinical studies have reported that radiolucent lines, associated with increased incidence of aseptic loosening, are most frequently observed at the rim of the superior acetabular quadrants [9,10], zone 1, which corresponds to the location where our model predicted higher cement mantle stresses.

In this study we considered a 50mm cemented acetabular cup. We recognise that not all brands will provide a 36mm option within a 50mm cup, many start at 54mm. If a 54mm cup would have been used for all measurements this would mean that cup thickness would effectively increase compared to the 50mm cup for all femoral head sizes tested in our investigation. In this case we would expect that the increase in cup thickness would help to better distribute the stress in the acetabular component thus resulting in lower stresses in the cement mantle, a finding which has been reported in the literature previously [12, 13].

In summary, our study has investigated the effect of using large femoral head sizes on stresses in the acetabular cement mantle and pelvic bone following THA. Whilst pelvic bone stress remained relatively invariant to femoral head implant size, stress on the cortical bone-cement interface increased with femoral head diameter by up to 9%. The largest stresses occurred in the anterosuperior and posterosuperior regions of the bone-cement interface,

where debonding usually initiates. We also found that stresses on the cement mantle interfaces increased by 100% when body weight went from 700N to 1000N. This suggests that the use of cemented acetabular cups for higher weight patients should be carefully examined and that where they are used it may be beneficial to use femoral head sizes of less than 36mm in these cases. Our findings may help to explain higher joint failure rates associated with larger femoral heads.

**Acknowledgements**

The authors would like to thank the Consejo Nacional de Ciencia y Tecnología (Mexico) for supporting the postgraduate student involved in this work.

**References**

[1] No authors listed. 2014. 12th Annual Report. National Joint Registry of England, Wales and Northern Ireland. Hemel Hempstead, United Kingdom.

[2] No authors listed. 2017. 14th Annual Report. National Joint Registry of England, Wales and Northern Ireland. Hemel Hempstead, United Kingdom.

[3] No authors listed. 2013. 10th Annual Report. National Joint Registry of England, Wales and Northern Ireland. Hemel Hempstead, United Kingdom.

[4] Triclot P, Gouin F. 2011. Update-"Big-head": The solution to the problem of hip implant dislocation?. Orthopaedics & Traumatology: Surgery & Research. 97(4): S42-8.

[5] Stroh DA, Issa K, Johnson AJ, Delanois RE, Mont MA. 2013. Reduced dislocation rates and excellent functional outcomes with large-diameter femoral heads. The Journal of Arthroplasty. 28(8):1415-20.

[6] Ramos A, Simões JA. 2009. The influence of cement mantle thickness and stem geometry on fatigue damage in two different cemented hip femoral prostheses. Journal of Biomechanics. 42(15):2602-10.

[7] Coultrup OJ, Hunt C, Wroblewski BM, Taylor M. 2010. Computational assessment of the effect of polyethylene wear rate, mantle thickness, and porosity on the mechanical failure of the acetabular cement mantle. Journal of Orthopaedic Research. 28(5):565-70.

[8] Bernoski FP, New AM, Scott RA, Northmore-Ball MD. 1998. An in vitro study of a new design of acetabular cement pressurizer. The Journal of Arthroplasty. 13(2):200-6.

[9] Mueller LA, Nowak TE, Mueller LP, Schmidt R, Ehrmann C, Pitto RP, Pfander D, Forst R, Eichinger S. 2007. Acetabular cortical and cancellous bone density and radiolucent lines after cemented total hip arthroplasty: a prospective study using computed tomography and plain radiography. Archives of orthopaedic and trauma surgery. 127(10):909-17.

[10] Zicat B, Engh CA, Gokcen E. 1995. Patterns of osteolysis around total hip components inserted with and without cement. JBJS. 77(3):432-9.

[11] Tong J, Zant NP, Wang JY, Heaton-Adegbile P, Hussell JG. 2008. Fatigue in cemented acetabular replacements. International Journal of Fatigue. 30(8):1366-75.

[12] Lamvohee JM, Mootanah R, Ingle P, Cheah K, Dowell JK. 2009. Stresses in cement mantles of hip replacements: effect of femoral implant sizes, body mass index and bone quality. Computer methods in biomechanics and biomedical engineering. 12(5):501-10.

[13] Hua X, Li J, Wang L, Wilcox R, Fisher J, Jin Z. 2015. The effect of cup outer sizes on the contact mechanics and cement fixation of cemented total hip replacements. Medical Engineering and Physics. 37(10):1008-14.

[14] Hua X, Wroblewski BM, Jin Z, Wang L. 2012. The effect of cup inclination and wear on the contact mechanics and cement fixation for ultra high molecular weight polyethylene total hip replacements. Medical Engineering and Physics. 34(3):318-25.

[15] Crowninshield RD, Maloney WJ, Wentz DH, Humphrey SM, Blanchard CR. 2004. Biomechanics of large femoral heads: what they do and don't do. Clinical Orthopaedics and Related Research. 429:102-7.

[16] Hoeltzel DA, Walt MJ, Kyle RF, Simon FD. 1989. The effects of femoral head size on the deformation of ultrahigh molecular weight polyethylene acetabular cups. Journal of biomechanics. 22(11):1163-73.

[17] Dunne N, Clements J, Wang JS. 2014. Acrylic cements for bone fixation in joint replacement. In: Revell P.A. Joint Replacement Technology, 1st ed. Woodhead Publishing; p 212-256.

[18] Kühn K.D. 2005. What is bone cement? In: Breusch, Malchau. The well-cemented total hip arthroplasty, 2005 ed. Berlin Heildelberg: Springer; p 52-59.

[19] Ghosh R, Gupta S, Dickinson A, Browne M. 2013. Experimental validation of numerically predicted strain and micromotion in intact and implanted composite hemi-pelvises. Proceedings of the Institution of Mechanical Engineers, Part H: Journal of Engineering in Medicine. 227(2):162-74.

[20] Ghosh R, Pal B, Ghosh D, Gupta S. 2015. Finite element analysis of a hemi-pelvis: the effect of inclusion of cartilage layer on acetabular stresses and strain. Computer Methods in Biomechanics and Biomedical Engineering. 18(7):697-710.

[21] Alonso-Rasgado T, Jimenez-Cruz D, Bailey CG, Mandal P, Board T. 2012. Changes in the stress in the femoral head neck junction after osteochondroplasty for hip impingement: a finite element study. Journal of Orthopaedic Research. 30(12):1999-2006.

[22] Bergmann G, Graichen F, Rohlmann A, Bender A, Heinlein B, Duda GN, Heller MO, Morlock MM. 2010. Realistic loads for testing hip implants. Bio-medical Materials and Engineering. 20(2):65-75.

[23] Aramis User Manual, 2009. GOM, Germany.

[24] Dalstra M, Huiskes R. 1995. Load transfer across the pelvic bone. Journal of Biomechanics. 28(6):715-24.

[25] Faris PM, Ritter MA, Keating EM, Thong AE, Davis KE, Meding JB. 2006. The cemented all-polyethylene acetabular cup: factors affecting survival with emphasis on the integrated polyethylene spacer: an analysis of the effect of cement spacers, cement mantle thickness, and acetabular angle on the survival of total hip arthroplasty. The Journal of arthroplasty. 21(2):191-8.

[26] Lichtinger TK, Müller RT. 1998. Improvement of the cement mantle of the acetabular component with bone cement spacers. Archives of orthopaedic and trauma surgery. 118(1-2):75-7.

[27] Zijlstra WP, De Hartog B, Van Steenbergen LN, Scheurs BW, Nelissen RGHH. 2017. Effect of femoral head size and surgical approach on risk of revision for dislocation after total hip arthroplasty. Acta Orthop. 2017 Aug;88(4):395-401. doi: 10.1080/17453674.2017.1317515. Epub 2017 Apr 25.

**Tables**

Table 1 Comparison of FE model predictions and experimental results: average vertical surface strain (absolute) at the superior periacetabular region A1 (A1-1, A1-2). The reported experimental strain data is the average of 10 measurement repetitions.

| Load (N) | Average Vertical Strain (Micro-Strain) | | | | | | Micro Strain |
|---|---|---|---|---|---|---|---|
| | Superior periacetabular region (A1-1) | | | Superior periacetabular region (A1-2) | | | |
| | FE Model | Experiment | Difference (%) | FE Model | Experiment | Difference (%) | |
| 1200 | 117 | 112 | 4 | 240 | 236 | 2 | |
| 1400 | 132 | 126 | 5 | 280 | 286 | 3 | |
| 1600 | 155 | 156 | 1 | 320 | 323 | 1 | |
| 1800 | 175 | 168 | 5 | 360 | 364 | 2 | |
| | | | | | | | |
| Surface Strain Pattern at 1800 N | Finite Element Model Prediction | | | Experimental Result | | | |

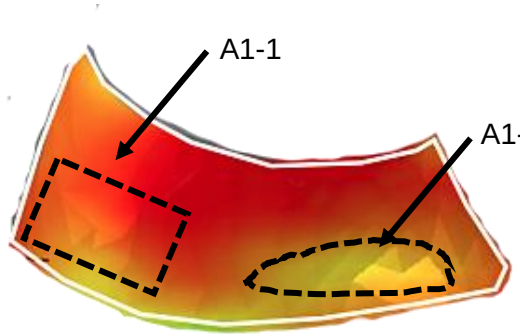


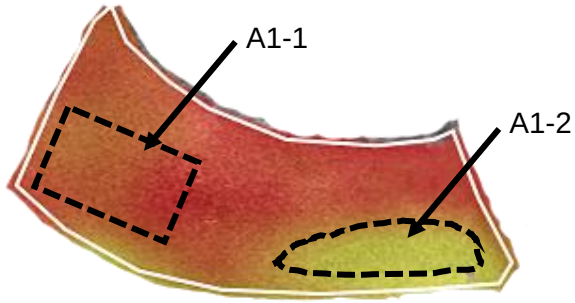


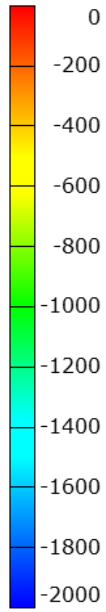

Table 2 Comparison of FE model predictions and experimental results: average vertical surface strain (absolute) at region A-2. The reported experimental strain data is the average of 10 measurement repetitions.

| Load (N) | Average Vertical Strain (Micro-Strain) | | | |
|---|---|---|---|---|
| | Superior periacetabular region (A2) | | | Micro Strain |
| | FE Model | Experiment | Difference (%) | |
| 1200 | 100 | 104 | 4 | |
| 1400 | 117 | 118 | 1 | |
| 1600 | 134 | 133 | 1 | |
| 1800 | 151 | 158 | 5 | |
| | | | | |
| Surface Strain Pattern at 1800 N | Finite Element Model Prediction 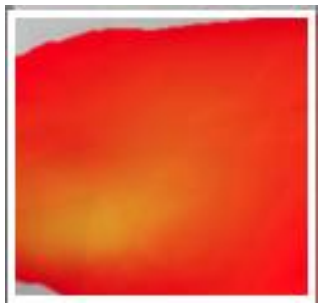 | | Experimental Result 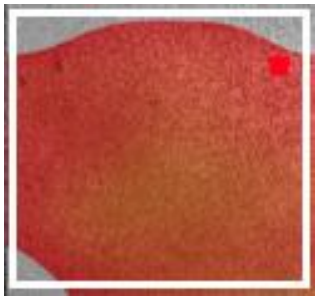 | 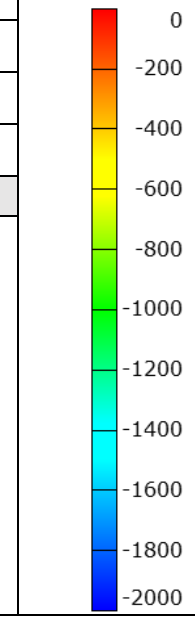  |

Table S-1 Mechanical properties.

| Material | Young's Modulus (MPa) | Poisson's Ratio (v) |
|---|---|---|
| Cortical bone | 16,000 | 0.3 |
| Trabecular bone | 155 | 0.3 |
| Acrylic bone cement | 2,000 | 0.3 |
| UHMWPE (Acetabular cup) | 800 | 0.4 |
| Steel (Femoral head) | 207,000 | 0.3 |

Table S-2 Number of tetrahedral and hexahedral elements for mesh sensitivity analysis.

| Number of Tetrahedral Elements (C3D10) | | | Hexahedral Elements (C3D20R) | | | | | |
|---|---|---|---|---|---|---|---|---|
| Mesh size | Part | | Part | | | | | |
| | Pelvic bone | Cement mantle | Head 28 mm | Cup 28 mm | Head 32 mm | Cup 32 mm | Head 36 mm | Cup 36 mm |
| Coarse | 105,091 | 11,743 | 160 | 448 | 312 | 448 | 432 | 448 |
| Medium | 162,389 | 15,862 | 704 | 2,336 | 896 | 1,752 | 1,840 | 1,168 |
| Fine | 207,162 | 21,210 | 1,600 | 5,180 | 2,976 | 4,144 | 3,456 | 3,108 |

Table S-3 Dimensions of the acetabular cup and femoral head for each of the three FE models.

| Model | Acetabular cup | | Femoral head |
|---|---|---|---|
| | Outer diameter (mm) | Inner diameter (mm) | Diameter (mm) |
| 1 | 50 | 36.5 | 36 |
| 2 | 50 | 32.5 | 32 |
| 3 | 50 | 28.5 | 28 |

## Figures

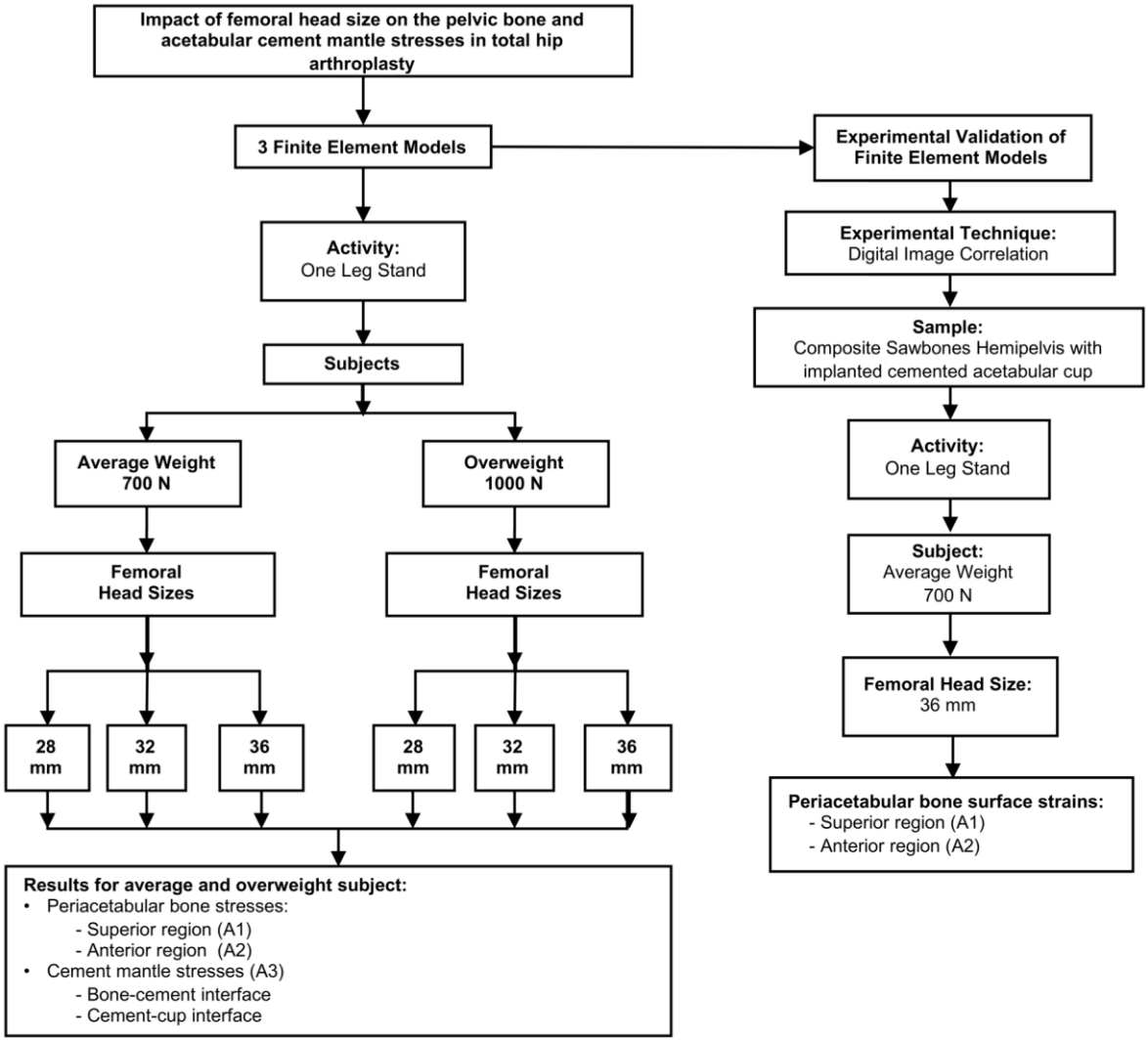


**Figure 1** Methodology flowchart

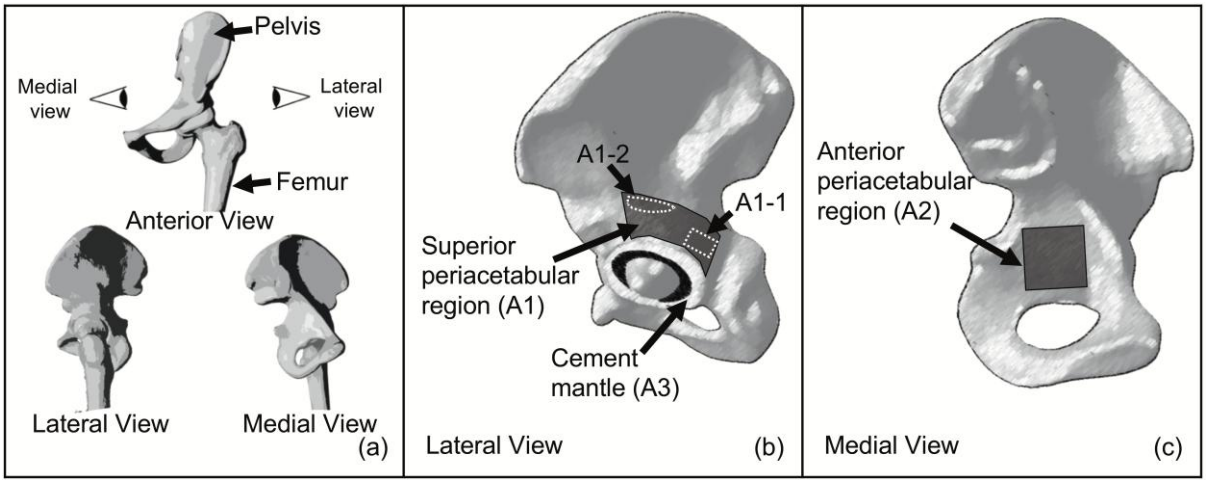


**Figure 2** Regions of interest. (a) Anterior, lateral and medial view of the hip joint, (b) lateral view of the hemipelvis showing regions A1(A1-1, A1-2) and A3, (c) medial view of the hemipelvis showing region A2.

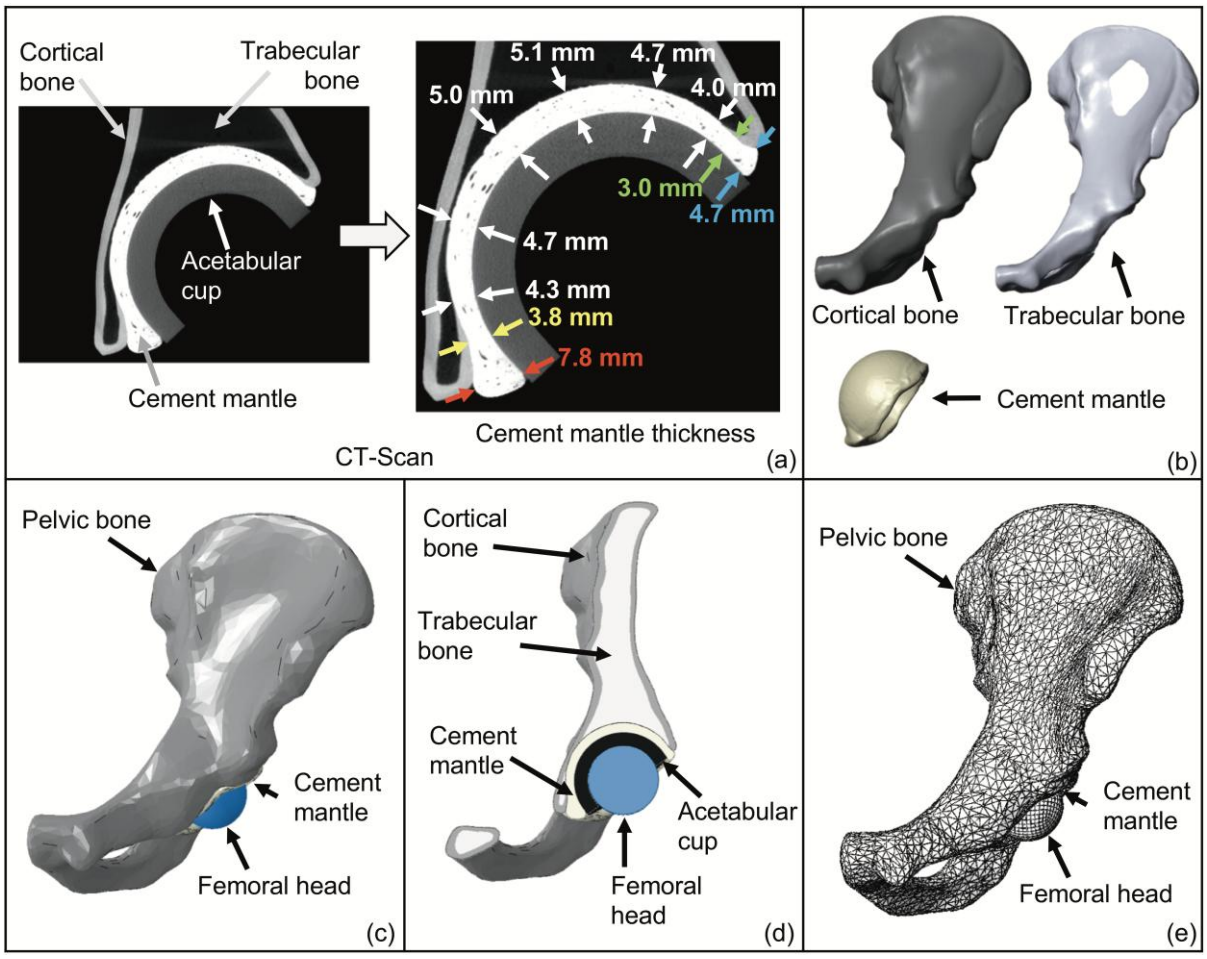


**Figure 3** Development of FE model. (a) CT slide of implanted hemipelvis showing a non-uniform cement mantle, (b) 3-D geometries (Scan IP) reconstructed from CT slices, (c) assembly of all model components (Abaqus 6.13), (d) transverse cut view of model assembly, (e) meshed assembly for FE analysis (Abaqus 6.13).

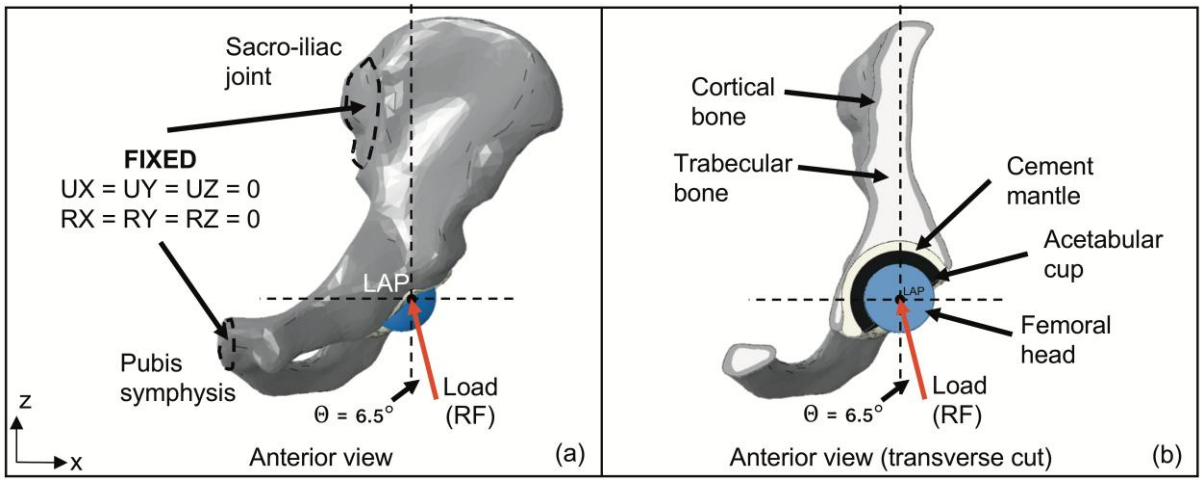


**Figure 4** Boundary conditions. (a) Anterior view of the hemipelvis showing the boundary conditions of the FE model, (b) transverse cut of anterior view of the hemipelvis showing all FE model parts.

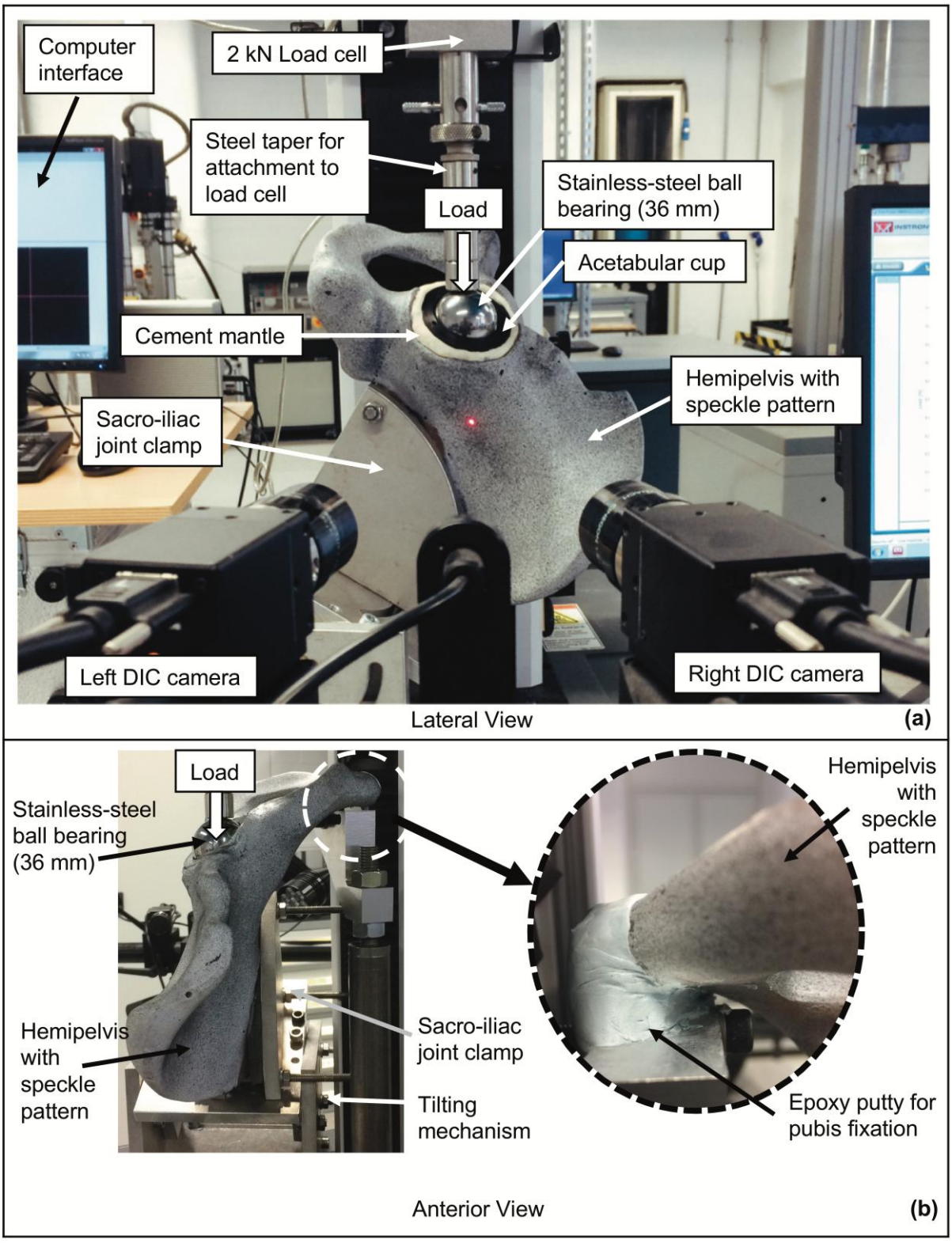


**Figure 5** Experimental setup for the application of the reaction force at the hip joint during one leg stance for the average subject. (a) Speckle pattern painted over the surface of the hemipelvis and the DIC cameras used to capture the data. (b) Fixation of the sacro-iliac joint and pubis symphysis.

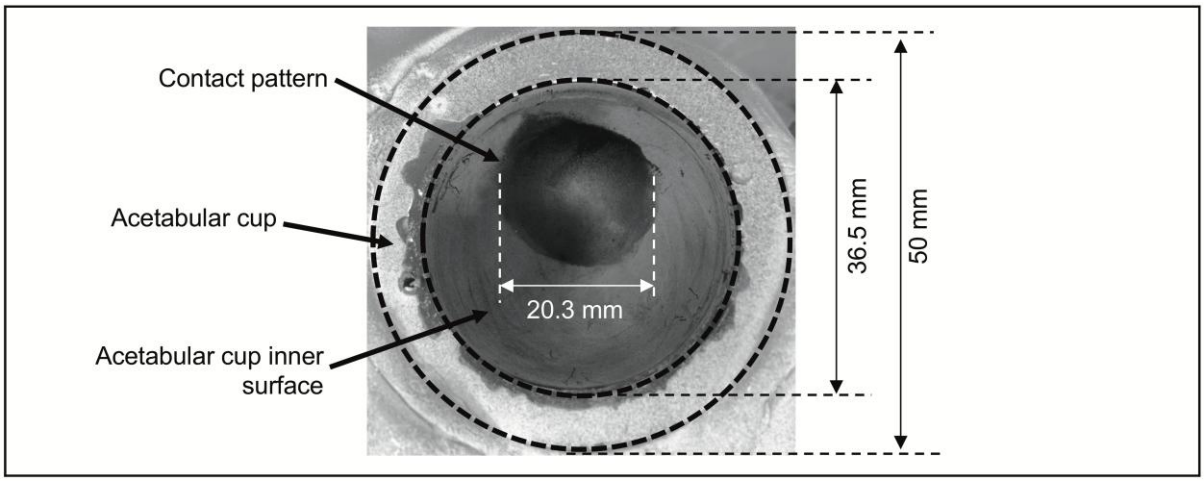


**Figure 6** Contact pattern between acetabular cup and stainless-steel ball bearing.

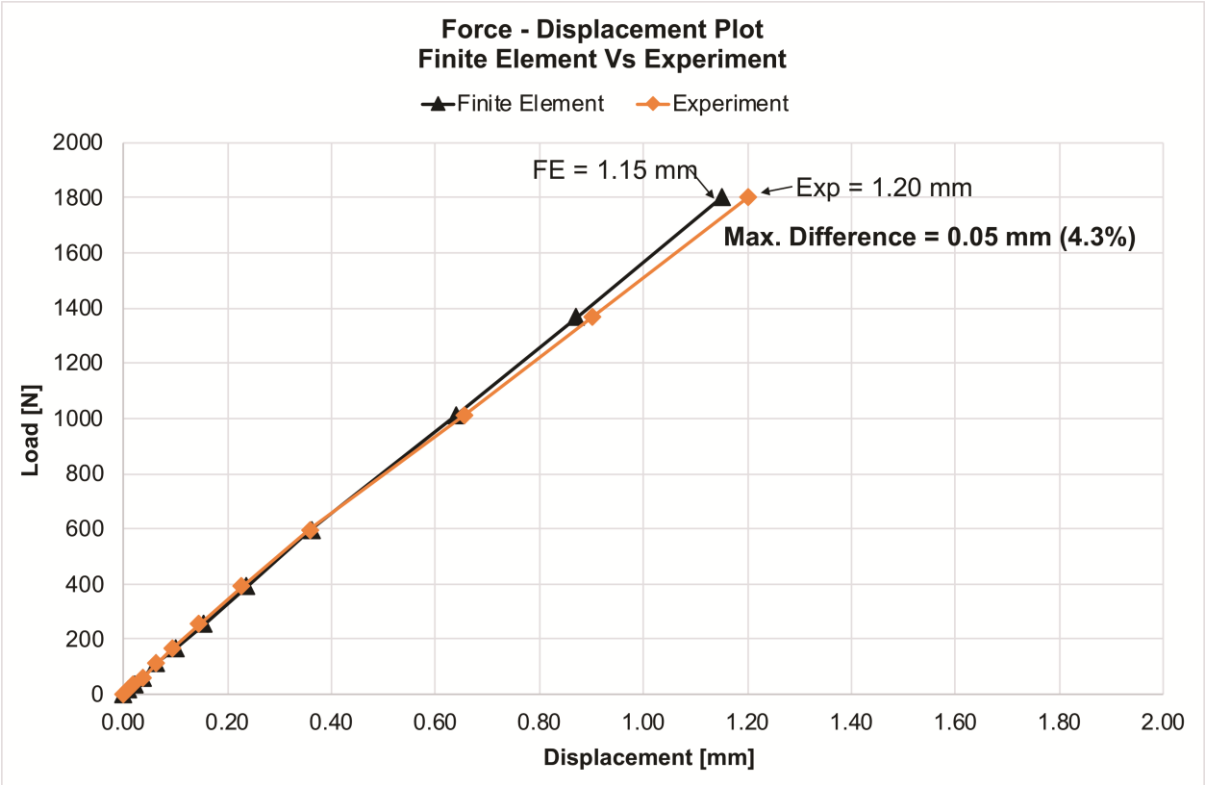


**Figure 7** Femoral head force-displacement curve for the numerical and experimental models.

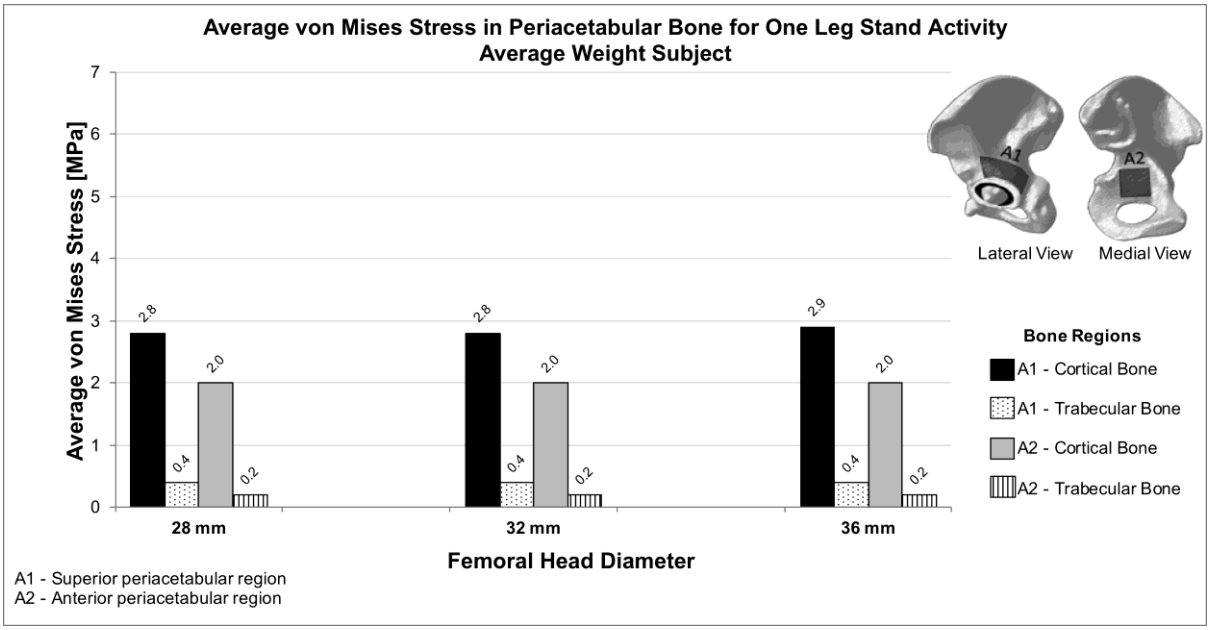


**Figure 8** FE model predictions of the average von Mises stress at the periacetabular bone regions A1 and A2 due to a reaction force (RF) of 1800 N at the hip joint during one leg stand activity for the average weight subject (700 N) for the 28 mm, 32 mm and 36 mm femoral heads.

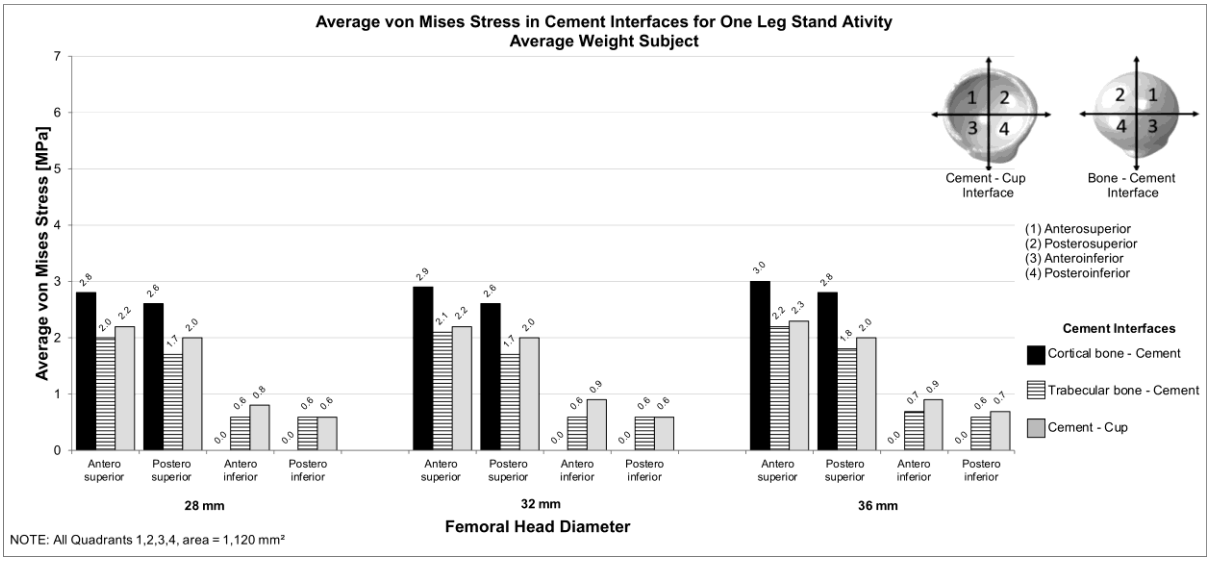


**Figure 9** FE model predictions of the average von Mises stress at the bone-cement and cement-cup interfaces due to a reaction force (RF) of 1800 N at the hip joint during one leg stand activity for the average weight subject (700N) for the 28 mm, 32 mm and 36 mm femoral heads.

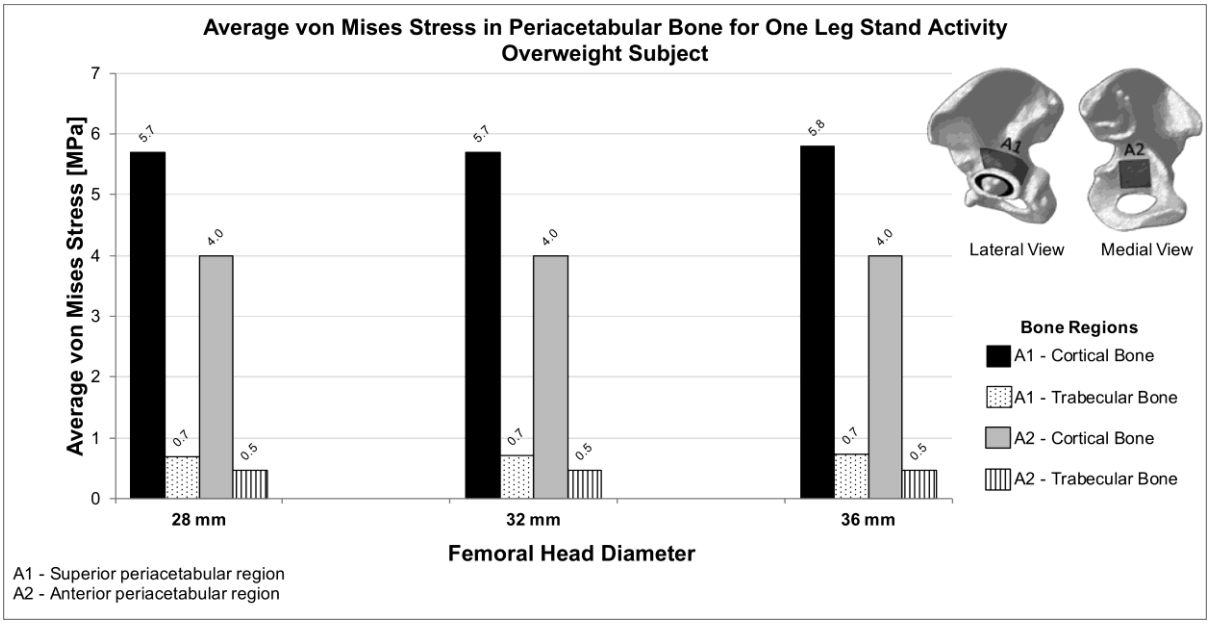


**Figure 10** FE model predictions of the average von Mises stress at the periacetabular bone regions A1 and A2 due to a reaction force (RF) of 3600 N at the hip joint during one leg stand activity for the overweight subject (1000 N) for the 28 mm, 32 mm and 36 mm femoral heads.

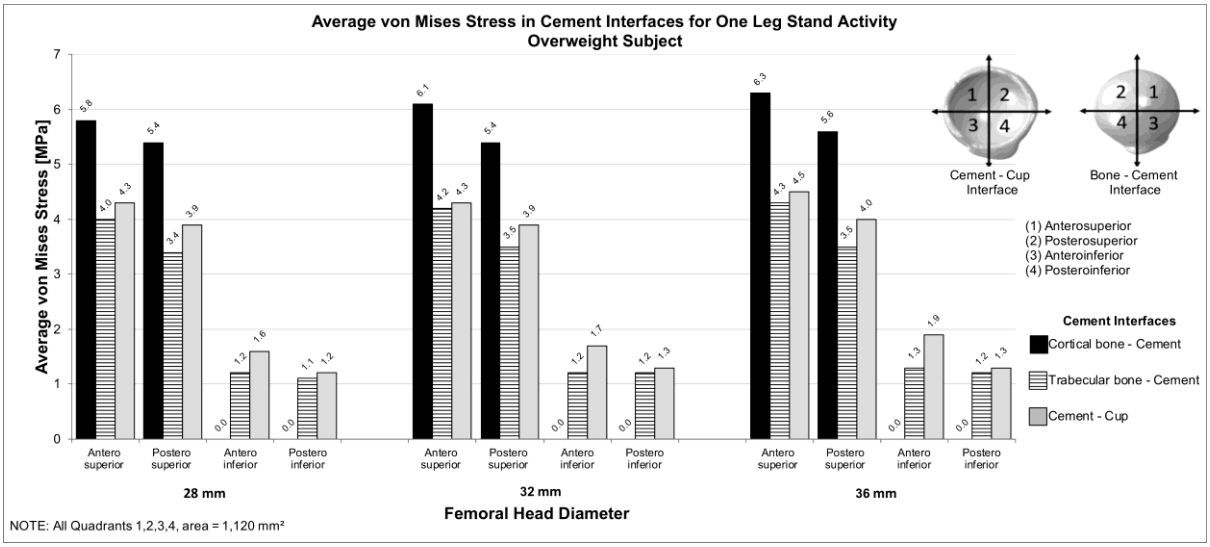


**Figure 11** FE model predictions of the average von Mises stress at the bone-cement and cement-cup interfaces due to a reaction force (RF) of 3600 N at the hip joint during one leg stand activity for the overweight subject (1000 N) for the 28 mm, 32 mm and 36 mm femoral heads.

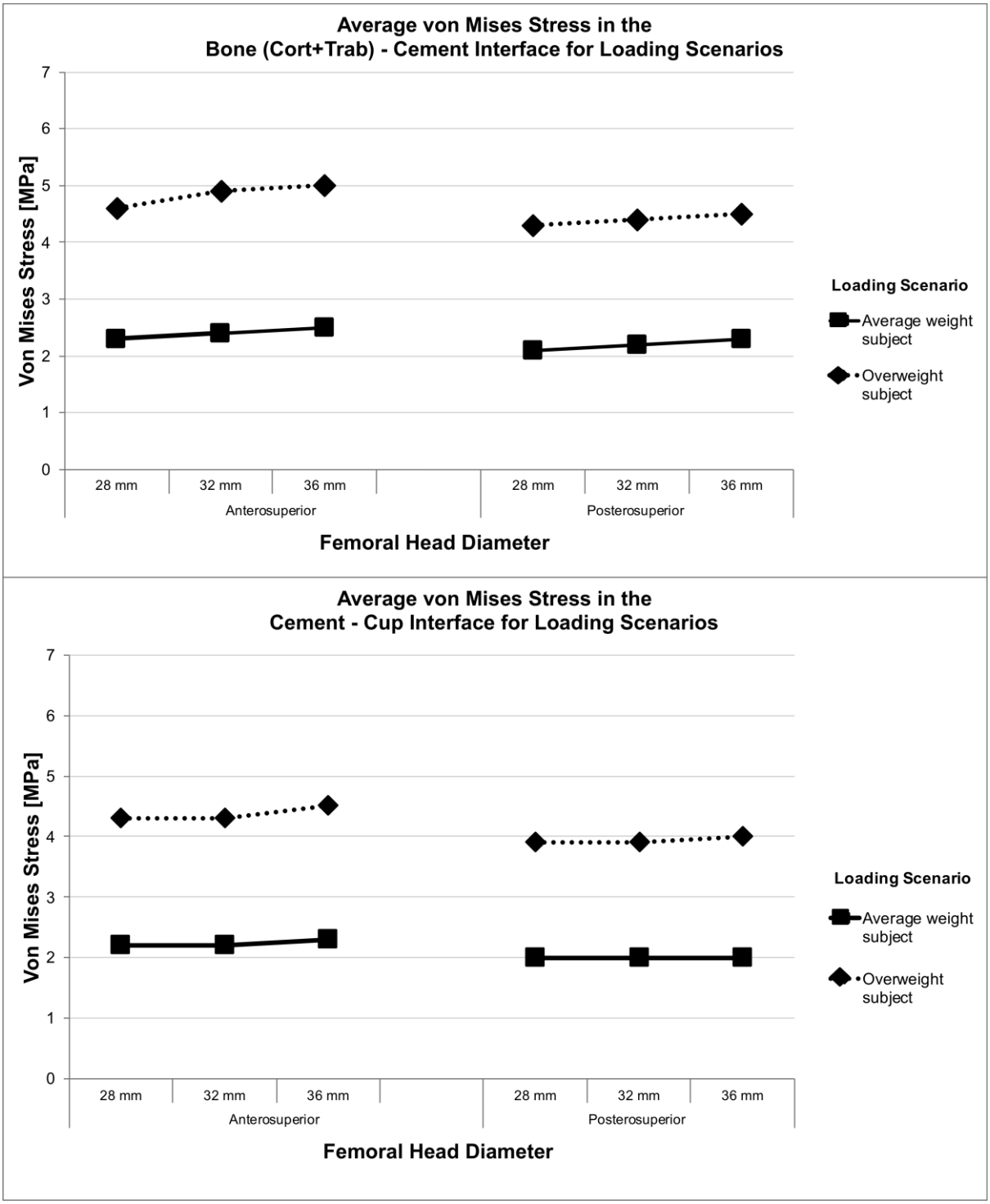


**Figure 12** Comparison of the average von Mises stress at the bone-cement and cement-cup superior interfaces during one leg stand activity for the average and overweight subjects for the 28 mm, 32 mm and 36 mm femoral heads.